

Hot corrosion mechanism of tundish plaster with steel slags in continuous casting

B. Malmal Moshtaghioun · Ahmad Monshi

Received: 4 September 2006 / Accepted: 22 December 2006 / Published online: 30 April 2007
© Springer Science+Business Media, LLC 2007

Abstract This study concerns the chemical reactions involved and the phases formed during penetration of slags of variable composition into porous plaster structure of tundish. Tundish plaster is mainly composed of MgO with minor amounts of SiO₂ and impurities, with a grain size of less than 1 mm, inorganic or organic fibers in order to decrease density and provide porosity for insulation, plasticizers and stiffening agents and some other additions. Tundish slag analysis for different grades of steel (7176D and 1191D, according to DIN standard) at different sequences, indicated a very variable composition of CaO (11–42%), SiO₂ (28–46%), Al₂O₃ (6–12%), MgO (11–20%), MnO (0–13%) and some minor variations of Fe, FeO and TiO₂. Experimental work indicated that slag when penetrated into pores of plaster, develop the phases of Monticellite (CaO · MgO · SiO₂) and Merwinite (CaO_{1.5} · MgO_{0.5} · SiO₂) around MgO particles and decrease the liquidus temperature from 2,800 °C to about 1,500 °C and provide dissolution of MgO grains in steel making process. Calculation based on two kinetic equations developed for diffusion controlled dissolution, indicated that the dissolution of MgO in tundish plaster is not a diffusion controlled process and is affected by turbulent flow parameters. Phase diagram of CaO–SiO₂–MgO indicates that decreasing SiO₂ to below 20% and increasing CaO content to as high as possible, increases the liquidus temperature to above 2,000 °C. Sources of SiO₂ in the

process are the rice husk addition, which is used as an insulating material on top of the melt, and the slag flux addition. These sources should be reduced to as low a level as possible. This fact does not affect the fluidity of slag which is required for inclusion removal. Fluidity of slag comes from low melting point eutectics in CaO–Fe₂O₃ and CaO–FeO (about 1,200 °C) due to iron oxide on top of the steel melt.

Introduction

Iron and steel making industries use about 70% of refractory production in the world [1]. Tundish and the disposable liner are important parts in the steel making process. Increased demands upon the performance and longer sequence life of the steel making tundish has driven a great number of changes in the sacrificial or expendable cover on permanent refractory brick or castable. This wear lining is called plaster of tundish and has a significant role in clean steel production.

There are a number of different types of tundish linings available in the market, such as ordinary plaster, gunnable, sprayable, board and recently in-situ formed dry system [2]. There are three major reasons why steel makers use coating materials to line the tundish rather than running directly on the permanent brick or castable back-up lining:

- Provide insulation by increasing the porosity inside the structure to preserve heat in the molten steel.
- Provide an inert barrier between the steel and back up lining to avoid any chemical reaction between the corrosive slag and the permanent refractory.
- Act as parting plane for easy descaling [3].

B. M. Moshtaghioun (✉) · A. Monshi
Department of Materials Engineering,
Isfahan University of Technology (IUT),
Isfahan 84156, Iran
e-mail: mmoshtagh@ma.iut.ac.ir

A. Monshi
e-mail: a-monshi@cc.iut.ac.ir

Tundish is not only a vessel for melt, but also a final stage of controlling the properties before continuous casting of steel [4]. Penetration of melt and slag into porous plaster causes sintering of this inert barrier and possible reaction with permanent liner. Dissolution of refractory material at the interface with slag is caused by some chemical reaction and or diffusion of reacting species into plaster [5]. The diffusion of FeO from slag into main refractory material of plaster, MgO, is first associated by formation of solid solution or magnesiowustite, (Mg,Fe)O [6]. The plaster usually is composed of the following [7, 8]:

- Basic refractory composition such as magnesia and olivine.
- Density reducing filler materials like inorganic or organic fibers (ceramic or glass fibers, paper fibers), expanded inorganic or organic materials (polystyrene beads), hollow ceramic microspheres [7], foaming agent (sodium lauryl sulfate), etc., or a combination of some of these lightweights, such as paper fibers and styrofoam beads [8].
- A plasticizer to enhance the ability of the composition to adhere to itself and the surfaces to which it is applied, such as silica fume.
- Some compositions can contain other additions like binder to promote initial gelling properties when mixed with water (alkaline earth phosphate or aluminum phosphate) and also imparting high temperature strength to the composition.
- The modifying agent can also be added to control the gelling properties of the binder, thus imparting a practical residence time to the composition. The set retarding agent provides a prolonged setting time (citric acid, tartaric acid, oxalic acid, malic acid).

On the other hand, slag is composed of different oxides. Basic tundish flux is also sometimes added on top of the tundish melt [9].

Slag reaction between the plaster material and tundish slag is of great importance especially when high sequence casts are required. Tundish slags in practice vary widely in composition, not only from shop to shop, but also during a single sequence. It is not unusual to have both a very acidic slag from the covering material most of the sequence and also have a very basic slag, possibly containing a lot of fluorspar, when ladle slag is carried over into the tundish. Thus, no one refractory composition will work best for all slag conditions. Basic materials, high in MgO with varied amounts of silica, are generally favored in the industrial applications [3].

The aim of this study is to investigate the reactions involved and the phases formed during penetration of slags of variable composition into porous plaster structure. Understanding the mechanism of phase formation and

evaluating low melting point products, leads to use of suitable fluxes in metallurgical processing, better selection of plaster composition, and decreasing the corrosion of slag–plaster and increasing the life of plaster for longer sequences.

Materials and methods

In order to study the corrosion of plaster of tundish by slag in a steel company, the chemical composition of three different plasters were studied, which is shown in Table 1. Two kinds of steel specified as 7176D and 1191D, according to DIN standard, which were produced in a larger quantity in the steel company were selected for this study, the composition of these steels are given in Table 2. A tundish fluxing powder was used for top of the steel melt in tundish for protection of the melt from oxidation and increase the capability of inclusion absorption. The composition of this fluxing powder is given in Table 3. This is a low melting point powder to develop a low viscosity slag on top of the melt and must contain some amounts of magnesia to saturate the artificial slag formed with MgO, in order to decrease the rate of dissolution of plaster material into this slag. In addition to this artificial slag, usually some burned rice husk is also added on top of steel melt to decrease the heat loss from the melt. The rice husk is a source of silica and increases the SiO₂ content of the slag formed.

Due to some variations in fluxing powder addition, rice husk addition, some slag coming from metallurgical processing through the ladle to the tundish, and more important than these, the gradual corrosion of plaster of tundish which converts refractory into the slag, the overall slag produced on top of the steel melt in the tundish has a variable chemical analysis in different sequences of use. Each sequence is defined as one melt coming from one specific ladle into the tundish and the numbers of sequences illustrate how many ladles have introduced their melt into the tundish so far in the continuous casting of steel. Table 4 shows the slag analysis of tundish for different grades of application. It must be mentioned that, this is the corrosion rate of expendable plaster of tundish that determines how many sequences can be used for a specific tundish and the steel producer wishes to increase the number of final sequences as far as possible, before interruption of the continuous casting process. In order to study corrosion mechanism of plaster of tundish and penetration of the viscous slag into the plaster, scanning electron microscopy (SEM) was used for observation of the penetration in the microstructure and energy dispersive spectroscopy analysis (EDS) was employed to have microanalysis of different parts of microstructure. This

Table 1 Chemical composition and physical properties of three different plasters of tundish

		Plaster M	Plaster P	Plaster T
Chemical analysis (%)	MgO	85.0	85.3	90–91
	SiO ₂	5.0	6.0	3
	Fe ₂ O ₃	–	1.5	<1
	Al ₂ O ₃	–	1.4	<0.5
	CaO	–	1.9	2–3
Bulk density (gr/cm ³)		1.7	1.59	1.6–1.7
Grain size (mm)		0–1	0–1	0–1
Cold crushing strength (kg/cm ²) after drying or firing at temperature <i>T</i>		30 (<i>T</i> = 1,000 °C)	(<i>T</i> = 110 °C)	–
		60 (<i>T</i> = 1600 °C)	30 (<i>T</i> = 1,400 °C)	–
Temperature limit of application (°C)		1,750	1,750	1,700

Table 2 Chemical composition of two different grades of steel produced in steel company

Grade	C%	Si%	Mn%	P% ≤	S% ≤	Cr%
7176D	0.52–0.59	0.15–0.4	0.7–1	0.035	0.035	0.6–0.9
1191D	0.42–0.5	≤ 0.4	0.5–0.8	0.035	0.03	–

Table 3 Chemical analysis and some specifications of the fluxing powder used by the steel company

C total%	SiO ₂ %	Fe ₂ O ₃ %	Al ₂ O ₃ %	CaO%	MgO%	CaO/SiO ₂
7.19	9.63	1.93	1.84	50.43	21.24	5.24
Melting temperature = 1400–1500 °C						
Bulk density = 0.55–0.65 g/cm ³						

elemental analysis has been converted to oxide basis by some calculations, since the slag is composed of different oxides of the elements. These relative oxide contents are estimates based on EDS analysis of cations and oxygen. In order to study the phase formation in the slag and in the reaction between slag and plaster, X-ray diffraction (XRD) studies were performed. CuK_α radiation ($\lambda = 1.542 \text{ \AA}$)

composed of CuK_{α1} and CuK_{α2} radiation was employed in a Philips instrument.

Results and discussion

XRD analysis of the slag produced in sequence 5 of the grade 7176D steel (according to Table 4) is shown in Fig. 1. It is illustrated that the main developed phases are Merwinite (CaO_{1.5} · MgO_{0.5} · SiO₂), Monticellite (CaO · MgO · SiO₂), Diopside (CaO · MgO · (SiO₂)₂), calcium iron oxide (CaO · FeO · Fe₂O₃). The melting points of these phases are Merwinite (1,575 °C), Monticellite (1,498 °C), Diopside (1,342 °C) and calcium iron oxide ($\approx 1,600 \text{ °C}$). Since the melt temperature of liquid steel in continuous casting is around 1,600–1,700 °C, these phases are liquid at continuous casting and produce a melt of low viscosity, which can penetrate into pores of plaster. The manufacturer of plaster use light fibers to decrease the bulk density and increase the porosity. This is to provide insulation property and protect permanent layer of refractory of tundish at the expense of expendable plaster. Some fibers like pulp (paper fiber) and or polymer fibers are burned at

Table 4 Slag analysis of tundish for different grades of steel and different sequences of application

Grade	Sequence	MgO%	Al ₂ O ₃ %	SiO ₂ %	CaO%	Fe%	FeO%	MnO%	TiO ₂ %	(MgO% + CaO%)/SiO ₂ %
7176D	1	12.75	10.41	31.40	42.25	1.79	1.45	1.11	0.28	1.75
	2	17.32	6.04	36.28	25.15	5.82	5.56	9.08	0.30	1.17
	3	11.17	7.93	46.43	18.09	4.52	2.10	11.37	0.47	0.63
	4	13.07	12.01	28.55	42.70	1.63	0.89	0.67	0.42	1.95
	5	18.03	9.75	28.62	38.21	3.80	2.67	1.09	0.50	1.96
1191D	3	14.50	7.70	36.17	15.63	9.27	6.29	11.56	0.29	0.83
	4	15.10	7.65	40.75	15.30	5.38	3.99	11.41	0.34	0.75
	5	12.35	7.93	40.41	14.29	7.79	5.52	10.29	0.30	0.66
	6	14.35	8.55	43.02	14.50	5.34	3.60	11.79	0.35	0.67
	7	11.5	9.91	39.98	11.36	8.93	6.51	12.74	0.37	0.57

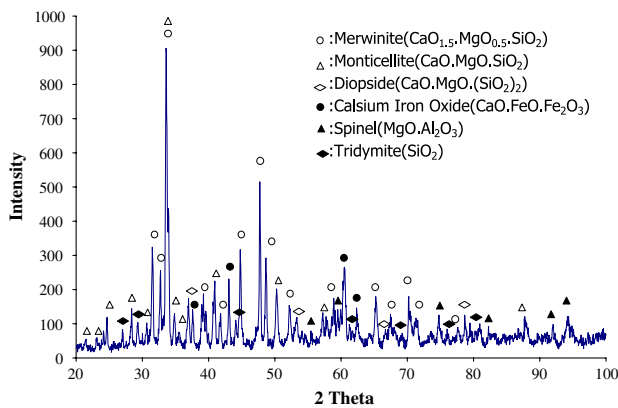


Fig. 1 XRD analysis of the slag produced in sequence 5 of the grade 7176D (According to Table 4)

high temperatures and changed into pores. Since plaster is made porous on purpose, it is natural for this low viscosity slag to penetrate into under layers of plaster and react with the MgO and provide the corrosion of the plaster by some chemical reactions. Merwinite ($\text{CaO}_{1.5} \cdot \text{MgO}_{0.5} \cdot \text{SiO}_2$), Monticellite ($\text{CaO} \cdot \text{MgO} \cdot \text{SiO}_2$), Diopside ($\text{CaO} \cdot \text{MgO} \cdot (\text{SiO}_2)_2$) can all be the products of such reactions. Tridymite (SiO_2) illustrate the presence of silica in the slag and Spinel ($\text{MgO} \cdot \text{Al}_2\text{O}_3$) confirms the reaction of alumina in the slag and magnesia in the plaster. Al ingot is introduced into the steel melt in metallurgical processing before pouring of melt into tundish from ladle. This is to absorb the oxygen content of the melt and produce mild steel. Al metal reacts with oxygen of the steel melt and converts to alumina. This alumina is inclusion of steel melt. During continuous casting, the flux which is rich in CaO as given in Table 3 is added on top of the melt in tundish to develop the required low viscosity slag and absorb the inclusion of Al_2O_3 from the melt. Slag analysis of 7176D grade steel in Table 4 shows that the flux has been added in sequence 1 and sequence 4. Alumina absorption is also rich in sequences 1 and 4. In sequences 2 and 3 the CaO and Al_2O_3 content gradually decrease, but SiO_2 content of slag is increased. This is due to the absorption of SiO_2 from under layer of rice husk which is used for insulation of the melt. The reaction between SiO_2 and CaO of slag with MgO of tundish plaster develop phases such as Merwinite, Monticellite and Diopside. The reaction between Al_2O_3 of slag with MgO of tundish plaster develops Spinel. Among all of these phases in slag, Spinel can be considered to have a positive role. This is because Spinel forms a passive layer on the surface of plaster which can protect against the progressive effect of corrosion to some extent.

Figure 2 shows the microstructure of plaster near the permanent layer before being in contact with melt and slag. It is shown that the structure is porous.

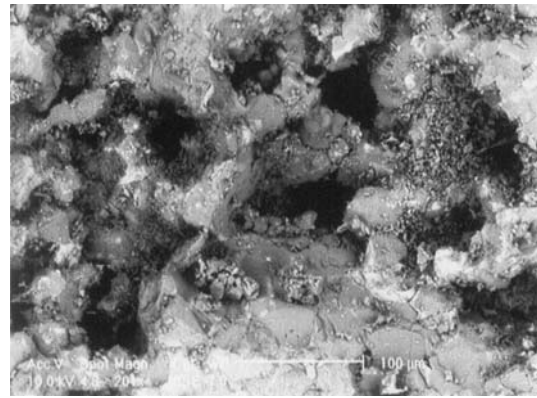


Fig. 2 SEM micrograph of plaster near the permanent layer before being in contact with melt and slag

Figure 3 shows the penetration of slag into pores of plaster and filling the pores and making contact with MgO grains in grade 7176D steel. This is an area near the slag–plaster interface after deskulling of the plaster.

Table 5 shows the EDS microanalysis of section shown in Fig. 3. Oxide calculations are estimates based on Elemental analysis of cations and oxygen performed by EDS. This analysis confirms the penetration of slag into MgO grains.

Figure 4 shows XRD phase analysis of the structure shown in Fig. 3. It gives the development of phases such as Fayalite ($(\text{Mg,Fe})\text{O}_2 \cdot \text{SiO}_2$), Merwinite ($\text{CaO}_{1.5} \cdot \text{MgO}_{0.5} \cdot \text{SiO}_2$), Monticellite ($\text{CaO} \cdot \text{MgO} \cdot \text{SiO}_2$) together with Spinel ($\text{MgO} \cdot \text{Al}_2\text{O}_3$) and primary grains of Periclase (MgO). The lower XRD analysis has shown the original unreacted plaster.

Figure 5 similarly illustrates the penetration of slag into pores of plaster in grade 1191D steel. This is also an area near the slag–plaster interface. Table 6 shows EDS

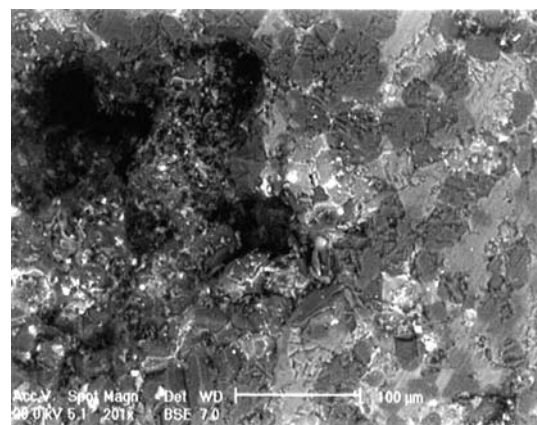
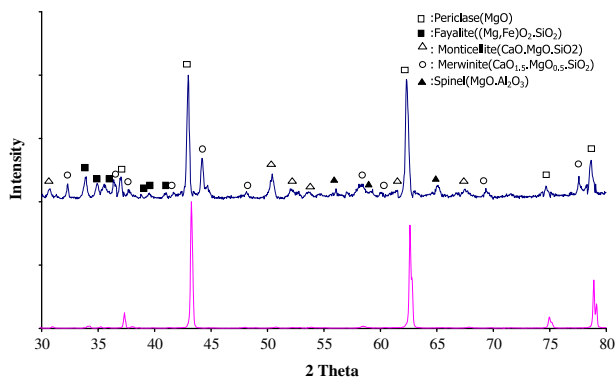
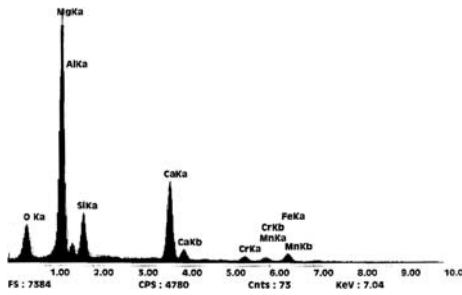
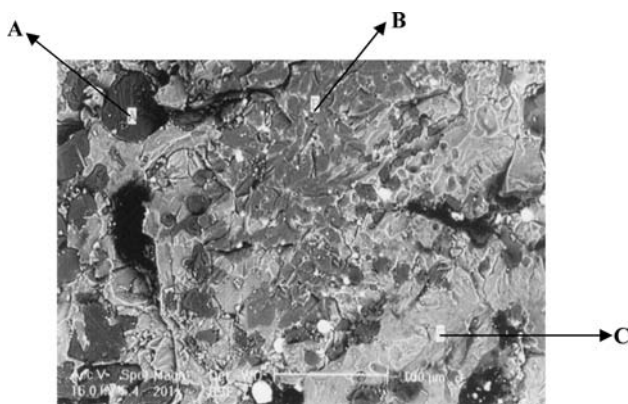


Fig. 3 Penetration of slag into pores of plaster in grade 7176D steel in right hand side of photograph near the slag–plaster interface. The left hand side shows porosity in plaster

Table 5 EDS microanalysis of Fig. 3 (penetration of slag into pores of tundish plaster)

Element	Mg	Al	Si	Ca	Cr	Mn	Fe
Weight%	47.83	1.37	6.30	25.43	2.43	2.02	5.78
Atomic%	54.46	1.41	6.21	17.56	1.30	1.02	2.91
Oxide	MgO	Al ₂ O ₃	SiO ₂	CaO	Cr ₂ O ₃	MnO	FeO
Mole%	65.21	0.84	7.44	21.02	0.77	1.22	3.48
Weight%	54.66	1.80	9.35	24.67	2.45	1.81	5.25

**Fig. 4** XRD phase analysis of the structure shown in Fig. 3**Fig. 5** Penetration of slag into pores of plaster in grade 1191D steel near the slag–plaster interface

microanalysis of Fig. 5. Table 7 gives the microanalysis of point A in Fig. 5, which is a MgO grain. Table 8 shows a chemical composition between MgO grain and the slag for point B in Fig. 5. It is believed that these are low melting point silicate phases such as Merwinite ($\text{CaO}_{1.5} \cdot \text{MgO}_{0.5} \cdot \text{SiO}_2$), Monticellite ($\text{CaO} \cdot \text{MgO} \cdot \text{SiO}_2$), which are formed on the surface of a MgO grain and EDS analysis gives information about the layer phases and some under

surface MgO particle. Table 9 shows a chemical composition high in CaO content and lower SiO₂ and MgO content. It is near to the slag composition and it confirms that point C in Fig. 5 is the penetration of slag into pores of plaster and coming into contact with MgO grains.

Figure 6 shows XRD phase analysis of the structure shown in Fig. 5. It gives the development of phases such as Fayalite ($(\text{Mg,Fe})\text{O}_2 \cdot \text{SiO}_2$), Cordierite ($\text{MgO}_2 \cdot (\text{Al}_2\text{O}_3)_2 \cdot (\text{SiO}_2)_5$), Merwinite ($\text{CaO}_{1.5} \cdot \text{MgO}_{0.5} \cdot \text{SiO}_2$), Monticellite ($\text{CaO} \cdot \text{MgO} \cdot \text{SiO}_2$) together with Spinel ($\text{MgO} \cdot \text{Al}_2\text{O}_3$) and primary grains of Periclase (MgO). The lower XRD analysis has shown the original unreacted plaster.

Table 5 shows the EDS analysis of Fig. 3, which is after sequence 5 for 7176D grade steel. Similarly, Table 6 indicates the EDS analysis of Fig. 5, which is after sequence 7 for 1191D grade steel. The main difference is a higher SiO₂ content in Table 6. It shows that by the increase of sequences, more SiO₂ can be absorbed from under layer of rice husk into slag. The XRD analysis of Fig. 6 (1191D) compared to Fig. 4 (7176D) shows similarity of phases Fayalite, Monticellite, Merwinite, Spinel, Periclase, and in addition Cordierite. Cordierite is a low melting phase ($T_m = 1,420^\circ\text{C}$) which is developed due to the presence of high amounts of SiO₂.

Points A, B and C in Fig. 5 are respectively microanalyses of dark region (MgO grain), gray region (silicate phases on the surface of MgO grain) and white region (slag phases). The EDS analysis for points A, B, C, respectively in Tables 7–9 can be used approximately for identification of these regions in Fig. 3.

The main oxide of tundish plaster is MgO, the main variable oxides of slag are acidic SiO₂ and basic CaO which provide acidic and basic overall compositions in different cases. Phase diagram of CaO–SiO₂–MgO is shown in Fig. 7 [10]. It was shown in Fig. 5 and the analysis of Table 8 that when slag is approached in contact with MgO grain, it has reacted on the surface of MgO grain and has developed phases such as Merwinite

Table 6 EDS microanalysis of Fig. 5 (penetration of slag into pores of tundish plaster)

Element	Mg	Al	Si	Ca	Mn	Fe
Weight%	34.66	2.20	17.14	31.82	1.82	2.84
Atomic%	39.72	2.27	17.00	22.12	0.92	1.42
Oxide	MgO	Al ₂ O ₃	SiO ₂	CaO	MnO	FeO
Mole%	48.25	1.37	20.65	26.69	1.12	1.72
Weight%	38.55	2.79	24.75	29.85	1.59	2.47

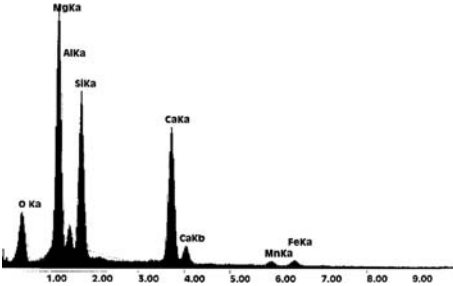


Table 7 EDS microanalysis of point A in Fig. 5

Element	Mg	Si	Ca
Weight%	90.49	0.99	2.42
Atomic%	88.61	0.84	1.44
Oxide	MgO	SiO ₂	CaO
Mole%	97.49	0.92	1.58
Weight%	96.45	1.36	2.19

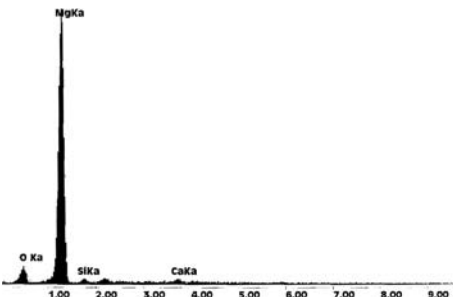


Table 8 EDS microanalysis of point B in Fig. 5

Element	Mg	Al	Si	Ca
Weight%	45.30	1.2	24.56	17.71
Atomic%	47.47	1.13	22.28	11.26
Oxide	MgO	Al ₂ O ₃	SiO ₂	CaO
Mole%	58.20	0.69	27.32	13.81
Weight%	48.39	1.46	34.07	16.07

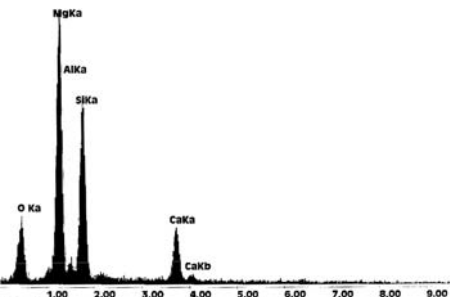
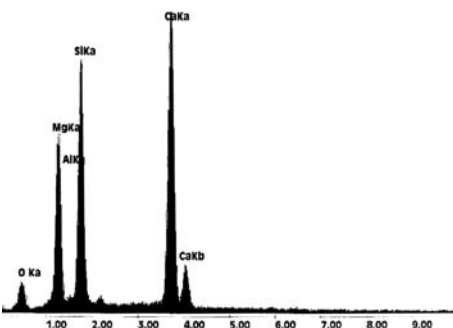


Table 9 EDS microanalysis of point C in Fig. 5

Element	Mg	Al	Si	Ca
Weight%	18.86	0.18	21.70	54.94
Atomic%	24.28	0.21	24.18	42.89
Oxide	MgO	Al ₂ O ₃	SiO ₂	CaO
Mole%	26.55	0.11	26.44	46.90
Weight%	20.09	0.21	30.01	49.68



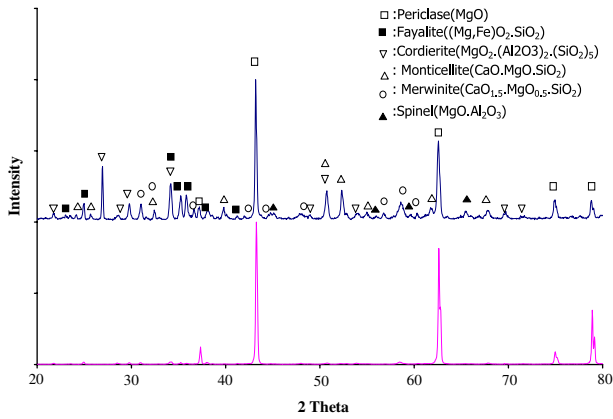
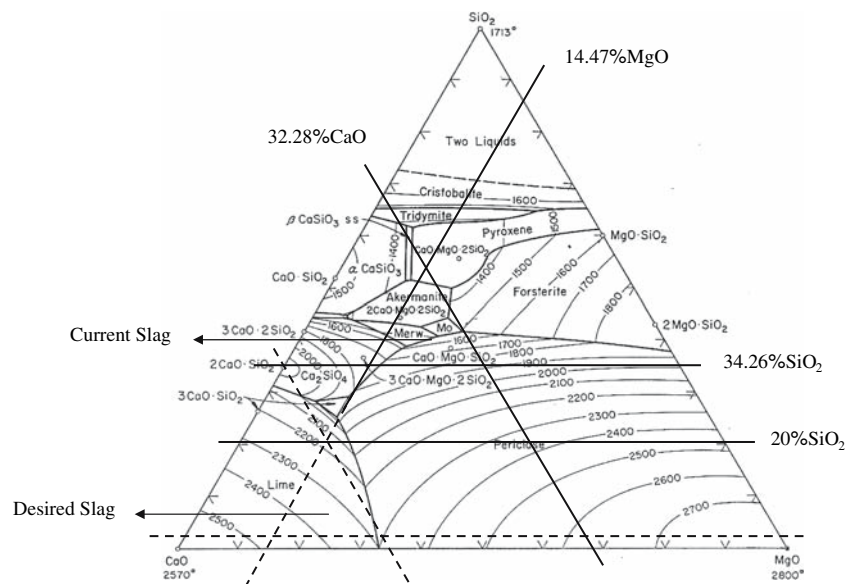


Fig. 6 XRD phase analysis of the structure shown in Fig. 5

($\text{CaO}_{1.5} \cdot \text{MgO}_{0.5} \cdot \text{SiO}_2$), Monticellite ($\text{CaO} \cdot \text{MgO} \cdot \text{SiO}_2$) around MgO grain. This is why EDS analysis indicate Mole fraction of about 14 CaO–27SiO₂–58MgO. The higher content of MgO is due to the penetration of X-rays under the surface layer of MgO grain and illustrates some analysis of the substrate in addition to the developed phases on the surface. Phase diagram shows how a melting point of 2,800 °C for MgO approaches the liquidus temperature of around 1,500 °C for these phases (Mo = Monticellite = 1,498 °C and Merw = Merwinite = 1,575 °C). Since the temperature of steel melt in tundish is around 1,600 °C or higher, these phases are melt and result the dissolution of MgO grains of tundish plaster. In order to avoid low temperature melting point phases that make hot corrosion of MgO grains, SiO₂ should be provided as low as possible and CaO as high as possible in the slag composition. Melting point of SiO₂ is 1,713 °C and that of CaO is 2,570 °C. If the overall content of SiO₂ in the tundish slag

goes under 20% and if possible under 10%, then the liquidus temperature in the CaO–SiO₂–MgO system is well above 2,000 °C. In order to illustrate the changes from current slag composition, which is a triangle with solid lines of 34.26% SiO₂, 32.28% CaO and 14.47% MgO to the desired composition which is shown by dashed lines in the phase diagram, the average values of SiO₂, CaO and MgO content of five different slags in 7176D (Table 4) is plotted in the phase diagram (Fig. 7) and the triangle by the intersection of these three lines is demonstrated at the central part of the diagram. The desired composition is shown by shifting the same size and shape of triangle to below 20% SiO₂ content and increasing the CaO content to balance this reduction, assuming MgO% is not changed. This triangle is shown in the lower left of the diagram. This means that the life time of tundish plaster is increased to longer sequences. Tundish slags should be liquid to assist inclusion removal, such as Al₂O₃ inclusion produced by reaction of oxygen in the steel melt with Al ingots added to the melt. By looking at flux composition in Table 3, it is understood that a high content of 50.43% CaO and only 9.63% SiO₂ is in the flux powder. This suggestion to increase CaO and decrease SiO₂ content of slag does not destroy the fluidity of slag. The main advantage of avoiding slag high in SiO₂ is that low melting point phases including MgO do not develop and MgO dissolution in slag is reduced. If the fluid slag high in CaO is present, then inclusion removal is performed and destructive phases with MgO are produced less. By referring to phase diagrams of CaO–Fe₂O₃ and CaO–FeO, it is understood that eutectics of around 1,200 °C develop and fluidity of CaO rich slag on top of steel melt is due to being associated with iron oxides. The source of SiO₂ in the tundish slag should be

Fig. 7 Phase diagram of the system CaO–SiO₂–MgO



avoided as much as possible. This should be concerned in metallurgical processing and flux addition. Also, the fired rice husk which is used for insulation purposes on top of liquid steel to keep the melt hot should be replaced by another insulation material low in SiO₂ and high in CaO content and insulating tundish powders should be designed to be used for these systems.

Recently, an article in the press [11], discusses direct and indirect dissolution of MgO particles in CaO–Al₂O₃–SiO₂ based slags and it is shown that boundary layer diffusion is responsible for the dissolution. The following equation based on shrinking core reaction models has been introduced as the satisfactory case:

$$\frac{R}{R_0} = \left(1 - \frac{t}{\tau}\right)^{1/2} \tag{1}$$

and

$$\tau = \frac{\rho R_0^2}{2D(C^{(p)} - C^{(s)})} \tag{2}$$

where R and R_0 are the actual and initial radius of the dissolving MgO particle, ρ is its density, t and τ are (the actual and total dissolution times respectively and $(C^{(p)} - C^{(s)})$ is the difference between the concentration of MgO in the slag (s) and the concentration of MgO in a saturated slag in equilibrium with the MgO particle (p). This concentration difference is the driving force for dissolving the MgO particle. D is the diffusion coefficient of the slowest diffusing species resulting from the dissolution process, which needs to be transported into the bulk slag across the boundary layer.

Another kinetic equation for diffusion controlled dissolution of refractory spherical particles in glassy melts is presented by Monshi [12] The kinetic equation is:

$$\ln \frac{m}{M} = -C \cdot \sqrt{t} \cdot e^{-\frac{A}{T}} \tag{3}$$

while M is the original amount (%) of refractory material (magnesia) in the system and m is the remained amount after passage of time t (in s or min or h) at absolute temperature of T . The constant C contains some physical properties like density of refractory particles and original size of particles in engineering raw material designed systems and balance of units on both sides of equation and a multiplication factor if the units of time are chosen as s, min, h, etc. The constant A informs about experimental activation energy (E) of diffusing species into particles of MgO.

Two practical experimental data of m_1 and m_2 at different temperatures of T_1 and T_2 with the same or different times of t_1 and t_2 are sufficient to evaluated the constants C

and A . The amount of M and m_1 and m_2 must be measured by one of the methods of quantitative X-ray diffraction analysis [13–15]. Solving two equations similar to Eq. 3 for two unknowns A and C yield the values of these two constants. The activation energy can be calculated as:

$$E = 2R \cdot A \tag{4}$$

while R is the gas constant. For isothermal firing of continuous casting, for example 1,600 °C (1,873 K), Eq. 1 simplification to

$$\ln \frac{m}{M} = \ln \frac{I}{I_0} = -H \cdot \sqrt{t} \tag{5}$$

where H is a constant containing temperature and includes both constants A and C . Then only one data m_1 for time t_1 and knowing M is sufficient to obtain H .

In order to compare two Eqs. 1 and 5 XRD results can be used. XRD results of Fig. 4 illustrates MgO peaks of original plaster (below) and the plaster used for 5 sequences each about 45 min for a total period of 225 min (top). Similarly XRD results of Fig. 6 are for 7 sequences (315 min).

It has been shown that [13–15] if I_{eij} is the diffracted intensity of set of phases, e in phase i in sample j:

$$I_{eij} = K_{ei} \frac{X_{ij}}{\mu_j^*} \tag{6}$$

while K_{ei} is a constant depending on the selected peak e and nature of the phases i and geometrical and electronical specifications of the XRD instrument. X_{ij} is the weight fraction of phase i in sample j and μ_j^* is the mass absorption coefficient of sample j being X-rayed. Since the selected plaster named P is similar in Figs. 4 and 6, which has been in contact with the slag at the same temperature of about 1,600 °C, for different soaking times of 225 and 315 min, respectively. The amounts of μ_j^* can be taken approximately similar in both cases and the values of the absolute peak heights can be related to the MgO amounts and the following relation may be used:

$$(I_{MgO})_{100} \approx C_1 \cdot X_{MgO} \tag{7}$$

This can be used for MgO₁₀₀ peak of original unreacted plaster and the other two cases.

Since the original particles of radius R_0 will be corroded to particles of radius R with the same density of ρ , therefore:

$$\frac{R}{R_0} = \left(\frac{\rho \cdot 4/3\pi R^3}{\rho \cdot 4/3\pi R_0^3}\right)^{1/3} = \left(\frac{X}{X_0}\right)^{1/3} = \left(\frac{I}{I_0}\right)^{1/3} \tag{8}$$

Table 10 Integrated intensity MgO_{100} peak of MgO phase

	Original values (I_0)	After time 225 min at 1,600 °C (I_1)	After time 315 min at 1,600 °C (I_2)
MgO_{100} peak at $d = 2.09 \text{ \AA}$	11299.70	5112.25	2430.49

Table 11 Calculation of constants from Eq. 1 to Eq. 5

Sample	Calculated τ	Calculated H
After time 225 min at 1,600 °C	547.9	0.0529
After time 315 min at 1,600 °C	491.4	0.0866

By using Eq. 1, the values of τ or the time required for completion of the corrosion of MgO particles in slag at 1,600 °C, are calculated from the data shown in the Table 10 and is given in Table 11. Some variations are observed in τ calculations and apparently Eq. 1 does not work for this system.

The same values of Table 10 are used to verify the H values of Eq. 5 and the results are given in Table 11. This relation also does not fit data. It can be concluded that the reaction of MgO dissolution in slag is not a diffusion controlled process. Turbulent flow of slag melts due to steel melt variations change the diffusion condition and change the kinetic behavior. Since the dissolution is not diffusion controlled, the phase formation also seems to be effected by non diffusion parameters. There is a chance of forming Spinel ($MgO \cdot Al_2O_3$) at the surface of MgO grains that may not be diffusion controlled and might change the kinetic behavior.

Conclusions

The main oxide of tundish plaster is MgO and tundish slag is variable in CaO and SiO_2 contents. Experiments indicated that slag, when penetrated into pores of plaster, develop the phases of Merwinite and Monticellite around MgO particles and decrease the liquidus temperature from 2,800 °C to about 1,500 °C and provide dissolution of

MgO grains in steel making process. Calculation based on two kinetic equations developed for diffusion controlled dissolution, indicated that the dissolution of MgO in tundish plaster is not diffusion controlled process and is affected by turbulent flow parameters. In order to increase the life time of plaster for longer sequences, the source of SiO_2 and CaO should decrease and increase respectively in metallurgical processing. Rice husk rich in SiO_2 for top of steel melt should be replaced by some tundish powder rich in CaO content. Phase diagram of CaO– SiO_2 –MgO system indicates that by decreasing SiO_2 to below 20%, liquidus temperature is above 2,000 °C in the system. This means that low melting point phases between slag and MgO are not produced and MgO dissolution in slag is reduced. This fact does not affect the fluidity of slag which is required for inclusion removal. Fluidity of slag comes from low melting point eutectics in CaO– Fe_2O_3 and CaO–FeO (about 1,200 °C) due to iron oxide on top of the steel melt.

References

- Kataoka SI (1993) Refractories of steel making in Japan, Unitcer 93 conf proc pp 1–27
- Connor G (2002) Chemically bonded tundish lining system and associated near tundish refractories, Foseco Steel International report
- Stendera JW (2002) Refract Appl News 7(6):26
- Mazumdar D, Guthrie RIL (1991) ISIJ Int 39:524
- Leasky LA, Mchale AE (1989) Ceram Trans 4:453
- Matsui T, Hiragushi K, Ikemoto T, Sawano K (2002) Taikabutsu 22(4):302
- Dody JA (1997) Lightweight sprayable tundish lining composition, US patent 5 602 063, 11 Feb. 1997
- Cheng JA (1991) Lightweight tundish refractory composition, US patent 5 073 525, 17 Dec. 1991
- Barker BJ (2001) Basic tundish flux composition for steelmaking, US patent 6 179 895 B1, 30 Jan. 2001
- Levine EM, Mc Murdie HF, Hall FP (1956) Phase diagram for ceramists. The American Ceramic Society, Inc., p 115
- Liu J, Guo M, Jones PT, Verhaeghe F, Blanpain B, Wollants P (2006) J Eur Ceram Soc
- Monshi A (1998) Inter Ceram 47(3):155
- Alexander LE, Klug HP (1948) Anal Chem 20:886
- Monshi A, Messer PF (1989) Proc. 42 of British Ceramic Society, pp 201–212
- Monshi A, Messer PF (1991) J Mater Sci 26:3623